Journal of Applied Polymer Science

Elaboration and relationships between structure and rheological properties of microtalc or nanotalc/polyamide composites

Quentin Beuguel, Julien Ville, Jérôme Crépin-Leblond, Pascal Médéric, Thierry Aubry
LIMATB, Equipe Rhéologie, Université de Bretagne Occidentale, UFR Sciences et Techniques, 6 avenue Victor le Gorgeu, CS 93 837, 29 238 Brest Cedex 3, France
Correspondence to: J. Ville (E-mail: julien.ville@univ-brest.fr)

ABSTRACT: This study focuses on the elaboration of nanocomposites processed by melt mixing of a polyamide 12 matrix and a hydrogel filled with synthetic talc particles. The systems are obtained by simultaneous mixing using either an internal mixer or a lab twin-screw extruder. The structure and rheological properties of synthetic talc/polyamide composites are compared with those of natural talc/polyamide microcomposites and modified montmorillonite/polyamide nanocomposites. A multiscale structure, composed of numerous nanometric particles but also few micrometric aggregates, is obtained for synthetic talc/polyamide composites. In terms of processability, the lab twin-screw extruder is more adequate than the internal mixer for the elaboration of synthetic talc/polyamide composites with relatively high filler volume fractions. For composites elaborated with the extruder, the percolation threshold, estimated from linear viscoelastic measurements, is close to 1, 6, and 11%, respectively, with modified montmorillonite, synthetic talc, and natural talc particles, in agreement with structural results. © 2015 Wiley Periodicals, Inc. J. Appl. Polym. Sci. **2015**, *132*, 42299.

KEYWORDS: composites; microscopy; polyamides; rheology; structure-property relations

Received 14 November 2014; accepted 2 April 2015
DOI: 10.1002/app.42299

INTRODUCTION

In the early 1990s, polymer-layered silicate nanocomposites have attracted great interest because they often exhibit a significant improvement of macroscopic properties compared to that of conventional microcomposites, as reviewed by Sinha Ray and Okamoto.[1] Indeed, addition of low volume fractions of anisotropic organoclay nanoparticles with a high aspect ratio in thermoplastic matrix can lead to the improvement of flame retardancy,[2–4] barrier properties,[5–7] thermal properties,[4,8] and mechanical properties.[8,9] Besides, it was shown that these properties are affected not only by the matrix/filler affinity but also by the degree of nanoparticles dispersion, which results from processing conditions.[10]

Montmorillonite is one of the most commonly used layered silicate for the preparation of nanocomposites because of its high cation exchange capacity, surface area, surface reactivity, and adsorptive properties. Among all layered silicate/polymer systems, organically modified montmorillonite/polyamide nanocomposites are certainly the most commonly studied ones.[9–17] Indeed, these nanocomposites have been shown to exhibit a very low solid volume fraction threshold due to the formation of a clay percolation network.[14] For example, the study of the linear and nonlinear mechanical properties of organically modified montmorillonite/polyamide 12 composites, elaborated with an internal mixer, shows the existence of a percolation threshold at a clay volume fraction of about 1%.[17] It was also observed in the melt-state rheological properties of these nanocomposites,[14] suggesting a possible relationship between melt-state and solid-state properties.

Micrometric lamellar natural talc particles are widely used, for many years, to reinforce thermoplastic matrices in the same business sector as polymer-layered silicate nanocomposites, for applications in domestic appliances or automotive industries.[18,19] Because of the lack of exchangeable cations at the surface of natural talc particles, a delamination process has been used to obtain particles, referred to as high aspect ratio particles,[20] with average thickness of hundreds of nanometers. Consequently, the performance of composites based on high aspect ratio natural talc particles cannot compete with those of modified montmorillonite/polyamide 12 nanocomposites.

More recently, an innovative and more efficient process, based on hydrothermal synthesis of talc nanoparticles, was proposed.[21–24] This process leads to the formation of a hydrogel filled with synthetic talc nanoparticles.[25] Synthetic talc nanoparticles mixed with a polyamide 6 by using a twin-screw extruder were shown to be well-dispersed in the polymer matrix, resulting in a Young's modulus higher than that of composites based on micrometric natural talc.[26]

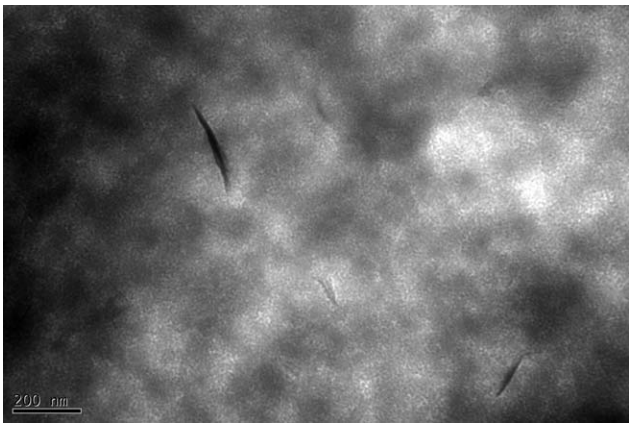

Figure 1. Transmission electron micrograph of hydrogel filled with ST particles diluted 10 times in water.

The aim of this study is to elaborate new polyamide 12 matrix nanocomposites filled with synthetic talc particles originally dispersed in a hydrogel, and to investigate their structure/rheology relationships. The main originality of the work is to compare these new synthetic talc/polyamide 12 composites to both natural talc/polyamide 12 microcomposites and modified montmorillonite/polyamide 12 nanocomposites, in terms of structural and rheological properties. Another original contribution of this work is the comparison of the feasibility and efficiency of two lab processing devices, an internal mixer and an extruder, to elaborate polyamide 12 matrix composites filled with synthetic talc particles originally dispersed in a hydrogel.

EXPERIMENTAL

Materials

The polyamide 12 (PA12) used as a matrix in this work is a commercial product, Rilsan® AECHVO, supplied by Arkema. The number and weight average molar weight were shown to be 38,000 and 60,000 g/mol, respectively, corresponding to a degree of polymerization of about 190, a radius of gyration of about 11 nm, and a polydispersity index close to 1.6. The melting point of this PA12 is 183°C, as determined by differential scanning calorimetry experiments with heating and cooling rates of 20°C/min. The weight loss was shown to be <0.5% after 45 min at 220°C, as estimated from thermogravimetric analysis. The Newtonian viscosity is close to 1300 Pa s at 200°C.

The hydrogel of Synthetic Talc (ST) particles was prepared at GET Laboratory (University Paul Sabatier, Toulouse, France) according to a hydrothermal process.[24] The specific area is about 150 m^2/g and the interlayer distance is 0.3 nm. The specific gravity of ST is 2.8. TEM micrograph of the hydrogel, diluted 10 times in water, is shown in Figure 1. The structure of hydrogel is composed of numerous small talc layer stacks but also a very small number of aggregates, with micrometric characteristic dimensions (from 1 to 5 μm). The average length of the nanotalc particles ranges from 30 to 3000 nm[25] and their thickness from 6 to 10 nm.

As mentioned above, structural and rheological properties of ST/PA 12 composites have been compared to those of layered silicate/PA12 nanocomposites and natural talc/PA12 conventional microcomposites:

- The layered silicate is an organically modified montmorillonite clay (OMMT), supplied by Southern Clay Products, namely Cloisite® C30B. It is a methyl tallow bis-2-hydroxyethyl ammonium exchanged montmorillonite clay, with a modifier concentration of 90 milliequivalent per 100 g. It has a good affinity toward polyamide.[14] This organophilic clay is characterized by a significant specific area ~700 $m^2\ g^{-1}$. The individual clay platelets are ~0.7 nm thick and ~200 nm long,[27] corresponding to an average ratio of 350. The interlayer distance, estimated from XRD measurements, is 1.2 nm and the specific gravity of OMMT is close to 2.
- The High Aspect Ratio® Natural Talc, referenced as HARNT in this article, is supplied by Imerys Talc. HARNT results from the delamination of coarser natural talc. The specific area is 19.5 m^2/g and the interlayer distance is close to 0.3 nm. The average equivalent diameter of these talc particles is about 2 μm when measured from sedimentation experiments and 10 μm when measured from laser diffraction experiments. The specific gravity of HARNT is close to 2.8.

Samples Preparation

First, PA12 was dried at 80°C for 4 h in vacuum because of the hygroscopic character of the matrix. All samples used in this study were prepared by simultaneous melt mixing of all components, using either Haake Rheocord internal mixer or DSM Xplore lab twin-screw extruder:

- The temperature imposed during mixing in internal mixer was 200°C and the mixing residence time was 6 min; the blade rotational speed was fixed at 100 rpm in internal mixer, corresponding to a characteristic shear rate of 135 s^{-1} according to the estimation by Bousmina *et al.*[28]
- The lab twin-screw extruder was operating at a barrel temperature of 220°C, corresponding to a melt temperature of ~200°C, for 6 min with a screw rotational speed of 50 rpm, corresponding to a maximum shear rate of about 750 s^{-1}, estimated from technical data.

After mixing, all samples were dried at 80°C for 4 h in vacuum and then pelletized. They were prepared for melt rheology by compression molding into 2-mm-thick plates, at 200°C; pressure was increased by steps, from 5 to 25 MPa, in order to avoid the formation of air bubbles during the compression process.

Following this route, samples were prepared at filler volume fractions, ϕ, ranging from 0 to 8.3%, 0 to 19.5%, and 0 to 11.3%, for OMMT, HARNT, and ST particles, respectively. It is worth pointing out that such volume fractions have been calculated from the weight fraction measured after calcination at 450°C in an oven, taking into account the organic content in the case of OMMT.

Structural and Rheological Characterization

The structure of the samples was investigated from 40-nm-thick ultrathin sections cut using a diamond knife, at −130°C, with

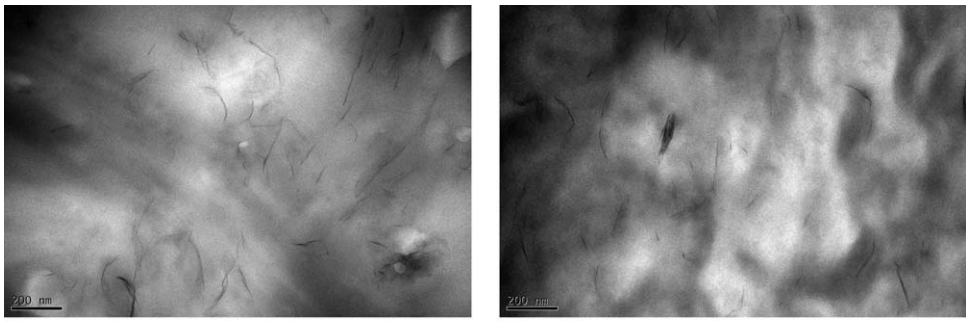

Figure 2. Transmission electron micrograph of weakly filled OMMT/PA12 nanocomposites mixed using (a) internal mixer and (b) twin-screw extruder with respective OMMT volume fraction of 1 and 0.5%.

an ultracryomicrotome (Reichert Jung); imaging was achieved with a JEOL 1400 Transmission Electron Microscope (TEM) at 100 kV. On TEM micrographs, length and thickness of fillers were measured for at least 200 particles, using SigmaScan® Pro 5.0 image analysis software. From these values, the number average length, L, and thickness, e, were calculated. The specific particle density, d_{sp}, that is the average number of particles per μm^2 divided by the filler weight fraction, as defined by Fornes *et al.*,[29] was also estimated. In order to complete TEM observations, cryofractured samples with vacuum-metallized surface were examined using a Hitachi S-3200N scanning electron microscope (SEM), with an accelerating voltage of 15 kV.

Oscillatory shear measurements were performed using a strain controlled rheometer (Gemini) equipped with parallel disks of 25 mm diameter and 2 mm spacing. All experiments were carried out at a temperature of 200°C, under a continuous purge of dry nitrogen in order to avoid sample degradation. Strain sweep tests have been systematically performed in order to determine the linear domain; all frequency sweep tests were performed at a strain amplitude within the linear viscoelastic regime.

RESULTS AND DISCUSSION

Structural Investigation

Figure 2 shows the typical TEM micrographs of OMMT/PA12 nanocomposite samples. The dark entities can be assigned to OMMT particles, illustrating that the degree of exfoliation is high, even if exfoliation seems to be imperfectly achieved either with the internal mixer [Figure 2(a)] or with the lab twin-screw extruder [Figure 2(b)]. Indeed, numerous individual clay particles and small few nanometers thick clay stacks are observed, as already reported by Aubry *et al.*[14] The measure of particles size, carried out from TEM micrographs, shows that the average particle length, $L = 65$ nm, is independent of OMMT volume fraction and of the mixing process (Table I).

On the contrary, the average particle thickness slightly increases with increasing OMMT volume fraction. This trend is clearly confirmed by the decrease of the specific particle density (Table I), explained by the presence of a few layer stacks, with a characteristic size of ~500 nm, in highly filled OMMT/PA12 nanocomposites.[10,14] It is also worth pointing out that the average thickness of OMMT particles, as well as the specific particle density, seems to be weakly dependent on the mixing device used in this study (Table I). The specific mixing mechanical energy, provided by both mixing devices in this study, is sufficiently high to lead to similar intercalation mechanisms, and therefore to almost identical clay particle structures. Indeed, the mechanical energy provided by the internal mixer, ~2300 kJ/kg, is four times higher than the critical mechanical energy estimated for OMMT/PA12 nanocomposites.[16]

Figure 3 presents the TEM micrographs of HARNT/PA12 composites, elaborated using either an internal mixer [Figure 3(a)] or a lab twin-screw extruder [Figure 3(b)]. Micrometric HARNT particles are observed in both micrographs. Most HARNT entities dispersed in PA12 matrix exhibit characteristic dimensions which are close to the values resulting from

Table I. Average Particle Length, L, Average Thickness, e, and Specific Particles Density, d_{sp}, for OMMT, HARNT, and ST Fillers

	Internal mixer				Twin-screw extruder			
	ϕ (%)	L (nm)	e (nm)	d_{sp} (part./μm^2)	ϕ (%)	L (nm)	e (nm)	d_{sp} (part./μm^2)
OMMT	1	~65	~4	19	0.5	~65	~4	23
	2.6		~5	11	2.6		~5	11
HARNT	1.8	~450	~60	< 0.2	1.9	~450	~55	< 0.2
	8.3				10.8			
ST	0.8	~65	~8	9	0.8	~65	~8	9
	2.1			7	2.2			7
	2.3			6	6.6			6

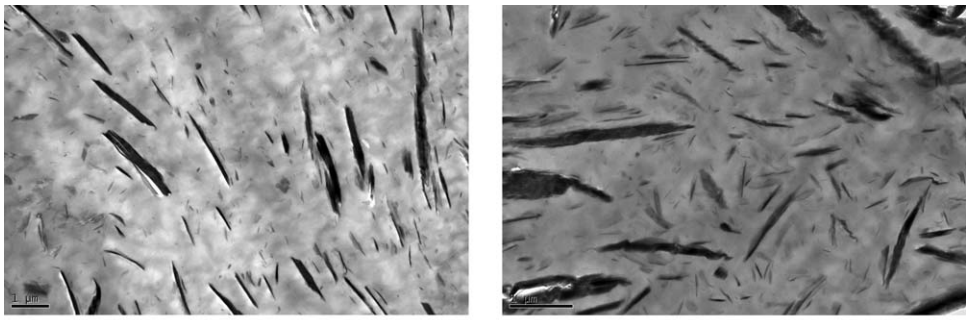

(a) (b)

Figure 3. Transmission electron micrograph of highly filled HARNT/PA12 microcomposites mixed using (a) internal mixer and (b) twin-screw extruder with respective HARNT volume fraction of 8.3 and 10.8%.

measurements carried out by sedimentation or laser diffraction techniques for the neat HARNT. TEM micrographs also reveal the presence of finer fillers, ~50 nm thick, probably due to a rip effect occurring during mixing. However, the average particle dimensions, as well as their specific density, which is inferior to 0.2 part/μm^2 (Table I), mean that HARNT/PA12 systems should be considered as microcomposites. Besides, HARNT volume fraction and the mixing device used have no significant effect on HARNT particle size, as shown in Table I.

Figure 4 presents the TEM micrograph [Figure 4(a)] and SEM micrograph [Figure 4(b)] of ST/PA12 composites, elaborated using either internal mixer or twin-screw extruder. A multiscale structure of ST particles in PA12 matrix was highlighted in Figure 4. Numerous fine ST particles and a few aggregates with submicronic thickness are well dispersed in the PA12 matrix [Figure 4(a)], for both melt-mixing processes used and all ST volume fractions investigated (Table II). However, a few micrometric aggregates and a very small number of almost millimetric agglomerates are evidenced by SEM technique [Figure 4(b)], from an ST volume fraction of ~2% incorporated into the internal mixer. The existence of few millimetric agglomerates, only at ~5% of ST (Table II), indirectly highlights the technological advantage of the twin-screw extruder for the elaboration of this kind of materials. We suggest that the fast drying of part of talc during its incorporation into the heated mixing device chamber leads to the formation of micrometric aggregates in the extrudate [Figure 5(a)] and of a whitish talc deposit on chamber wall and blade surface [Figure 5(b)]. The micrometric aggregated particles are difficult to disperse in the matrix, as illustrated by SEM micrograph of a microcomposite, elaborated from 3.1% dried synthetic talc (Figure 6). Moreover, the number of large particles increases with the incorporated talc fraction, highlighting that this harmful effect is more marked when the internal mixer is used. However that may be, the structure of ST particles is mainly characterized by the presence of individual ST particles and small stacks, leading to an average ST particle thickness, $e \sim 8$ nm, as reported in Table I. Such thickness value, which does not seem to depend on ST volume fraction and which is the same for both elaboration processes used in this work, is close to the one obtained for the ST-filled hydrogel (Figure 1), suggesting that there is no significant intercalation of PA12 matrix chains into the interlayer of ST particles, as confirmed by XRD results (not presented here). Moreover, despite the presence of a few aggregates in the PA12 matrix, the average length of ST particles, $L \sim 65$ nm, seems to be independent of ST volume fraction and of elaboration processes used in this study (Table I); it is close to the values

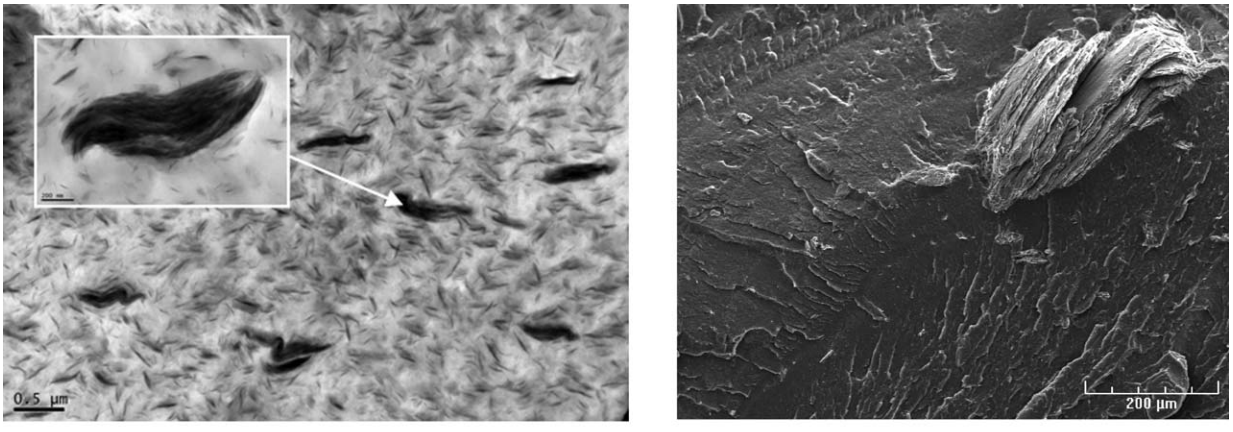

(a) (b)

Figure 4. (a) Transmission electron micrograph of 6.6% ST/PA12 composite mixed using twin-screw extruder and (b) scanning electron micrograph of 2.3% ST/PA12 composite mixed using internal mixer.

Table II. Typical Thickness of Various ST Entities and Clay Volume Fractions, with Either Internal Mixer or Twin-Screw Extruder

		Clay volume fraction	
	e (nm)	Internal mixer	Twin-screw extruder
Agglomerates	>100 μm	$\phi \sim 2\%$	$\phi \sim 5\%$
Aggregates	1–100 μm	$\phi \sim 2\%$	$\phi \sim 2\%$
Submicronic stacks	50 nm–1 μm	From the lowest volume fractions considered	
Layers and stacks	<50 nm		

obtained by Dumas *et al.*[25] It is also worth pointing out that ST and OMMT particles, with similar average length, exhibit comparable nanometric thickness, even though OMMT nanoparticles are slightly finer. However, in the case of ST/PA12 composites, the nanostructure is affected by the presence of micrometric aggregates and millimetric agglomerates (Table II), as underlined by a lower specific particle density (Table I).

Particle thickness distribution, determined from TEM micrographs, are given in Figure 7 for OMMT and HARNT fillers dispersed in PA12 matrix, at volume fractions of 1 and 8.3%, respectively. ST fillers thickness distribution in PA12 matrix is presented at volume fractions of 2.3 and 6.6% using internal mixer and twin-screw extruder, respectively.

Figure 7 clearly indicates that the thickness of OMMT particles does not exceed 50 nm. Let us note that the thickness distribution is broader with increasing OMMT volume fraction, because of the presence of few OMMT stacks, which lowers the specific particle density.[10] Figure 7 also shows a slightly broader thickness distribution when the internal mixer is used. However, the proportion of particles affected by the mixing device is very low, i.e., inferior to 10%, which could be explained by the relatively high mechanical mixing energy provided by both devices.[16]

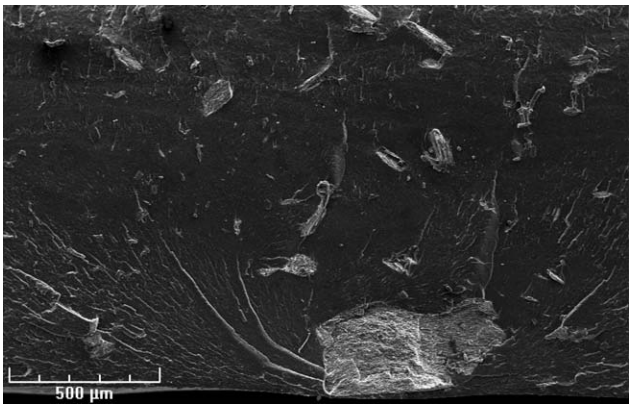

Figure 6. Scanning electron micrograph of microcomposite, elaborated from 3.1% dried synthetic talc.

Even without taking into account the significant quantity of micrometric aggregates, the thickness distribution of the HARNT particles is much wider than that of OMMT particles (Figure 7), highlighting the microcomposite character of HARNT/PA12 system.

The thickness distribution of ST particles is close to that of OMMT particles, at least until a cumulative frequency of ~80% (Figure 7). The remaining 20% correspond to stacks with thickness ranging from 50 nm to 1 μm. Nevertheless, the difference between both systems lies in the fact that the ST/PA12 composite is composed of aggregates (Table II), but also a very small number of millimetric agglomerates [Figure 4(b)] at high ST volume fractions (Table II). We would like to point out that the number density of these big entities is quite low, whereas their volume fraction is quite significant.

Using twin-screw extruder for PA12 matrix filled with 6.6% ST leads to a slightly narrower ST particle thickness distribution

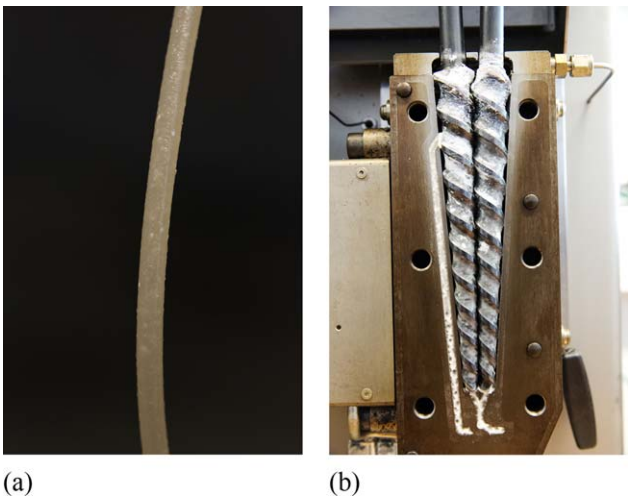

Figure 5. Highly filled 6.6% ST/PA12 composites camerawork: formation (a) of micrometric aggregates in the extrudate and (b) of a whitish talc deposit on chamber wall and blade surface. [Color figure can be viewed in the online issue, which is available at wileyonlinelibrary.com.]

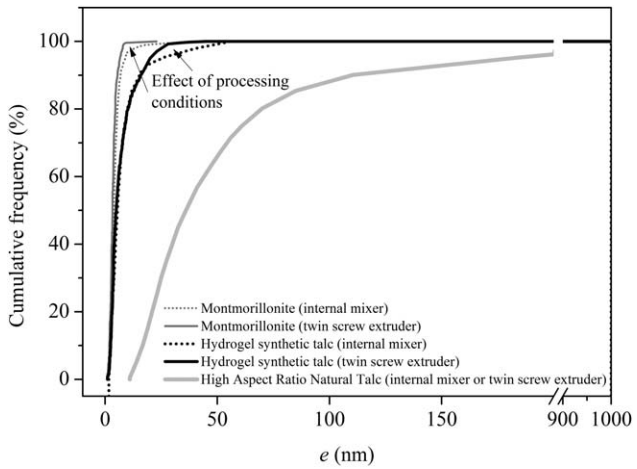

Figure 7. Particle thickness distribution for 1% OMMT/PA12 and 8.3% HARNT/PA12 composites using either internal mixer or twin-screw extruder. ST volume fraction is 2.3 and 6.6% using either internal mixer or twin-screw extruder, respectively.

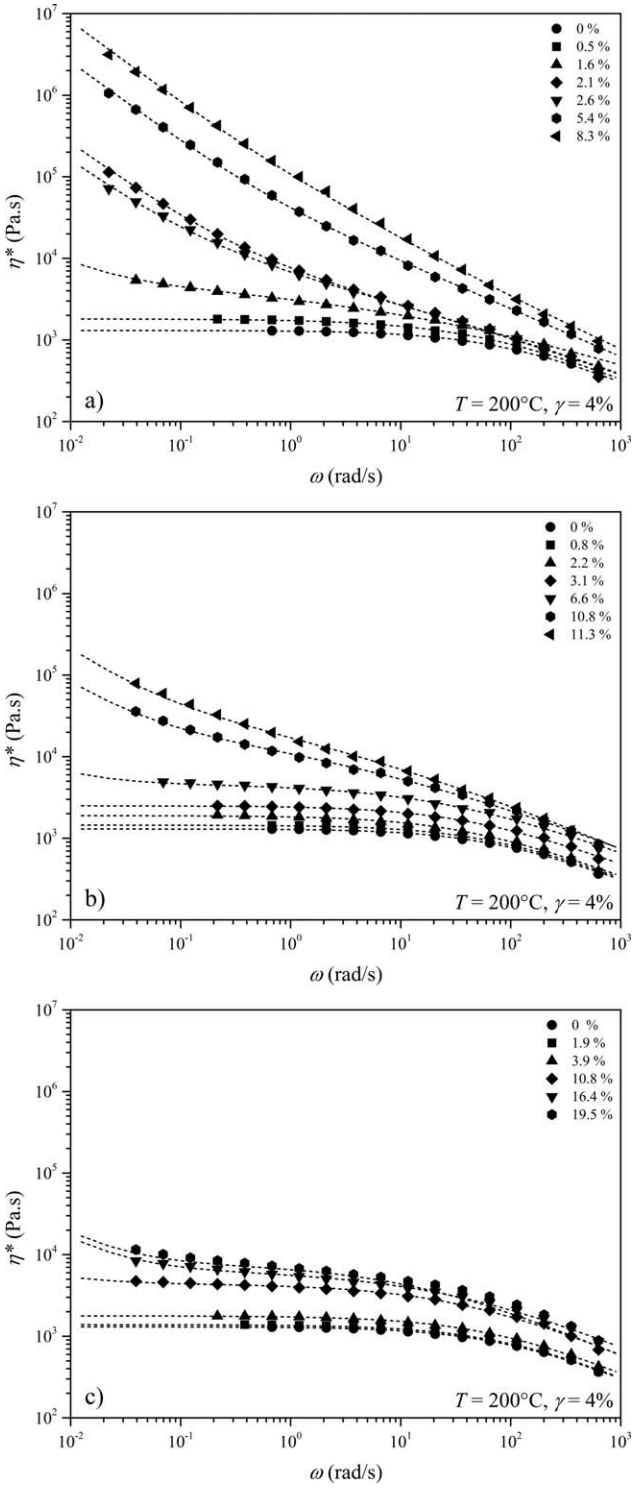

Figure 8. Complex viscosity as a function of angular frequency for (a) OMMT/PA12, (b) ST/PA12, and (c) HARNT/PA12 composites mixed using twin-screw extruder.

than using internal mixer for PA12 matrix filled with only 2.3% ST (Figure 7). In fact, only ~10% in number of finer ST particles are affected by this mixing process. On the other hand, the ST microstructure (aggregates and agglomerates) is not qualitatively influenced by the processing conditions (Table II).

In conclusion, results suggest that the structure of ST/PA12 composites is rather close to that of OMMT/PA12 nanocomposites; it is mainly constituted of nanometric particles, even if it is also composed of some micrometric and millimetric entities. Besides, the twin-screw extruder was shown to be more adequate than the internal mixer for the elaboration of synthetic talc/PA12 nanocomposites. The extruder slightly improves the nanostructure and leads to the formation of very large mineral particles at higher ST volume fractions. Moreover, the use of internal mixer presents some limits, in terms of processability, as compared to the lab twin-screw extruder:

- First, the incorporation of a relatively large amount of hydrogel with synthetic talc particles in the mixing chamber is delicate, leading to large losses of inorganic matter. These losses limit the preparation of ST-filled composites to volume fractions lower than only 3%. On the opposite, the twin-screw extruder is adequate for the preparation of ST/PA12 nanocomposites filled up to at least 11% ST.
- Second, the presence of micrometric aggregates and above all of millimetric agglomerates at weak ST volume fractions, ~2%, significantly affects these composites. By contrast, the twin-screw extruder leads to the formation of millimetric agglomerates at high ST volume fractions (~5%) only.

Therefore, the following part devoted to the rheological properties is limited to composites elaborated using twin-screw extruder only.

Rheological Investigation

Figure 8 shows the complex viscosity as a function of angular frequency, in the linear viscoelastic domain, for OMMT/PA12 nanocomposites, ST/PA12 composites, and HARNT/PA12 microcomposites, respectively.

The complex viscosity increases with increasing OMMT volume fraction, over the whole range of frequencies investigated. Up to a volume fraction Φ_p, nanocomposites present a Newtonian behavior at low frequencies, characterized by a Newtonian complex viscosity, η_0^*. Above Φ_p, nanocomposites exhibit a yield stress at low frequencies, attributed to the formation of a percolated network of OMMT nanoparticles.[14] For the OMMT/PA12 nanocomposites, the percolation threshold Φ_p, corresponding to the transition between Newtonian behavior and yield stress behavior, is close to 1%, as already reported for similar nanocomposites elaborated using an internal mixer.[10]

The complex viscosity also increases with increasing HARNT volume fraction, but the increase is less marked than that observed for OMMT particles. Contrary to OMMT/PA12 nanocomposites, no significant yield stress is observed at low HARNT volume fraction; only a slight increase of viscosity at low pulsations is observed for 10.8% HARNT.

In the case of ST/PA12 nanocomposites, Figure 8 also shows an increase of viscosity with ST content. More precisely, a Newtonian viscosity is measured for ST volume fractions lower than 6.6%. At higher ST volume fractions, a yield stress appears. As proposed for OMMT/PA12 nanocomposites, it could be attributed to the existence of a percolation network, due to the

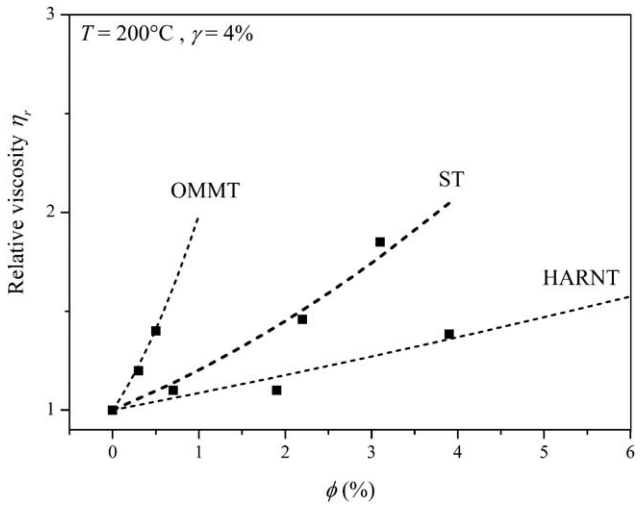

Figure 9. Relative viscosity as a function of fillers volume fraction for OMMT/PA12, ST/PA12, and HARNT/PA12 composites mixed using twin-screw extruder.

mainly nanometric structure of ST/PA12 composites, as shown in Figure 4(a). It is worth pointing out that the percolation volume fraction, ~6%, characterizing ST/PA12 nanocomposites is between that of HARNT/PA12 microcomposites and that of OMMT/PA12 nanocomposites, in agreement with structural results.

Below the percolation threshold Φ_p, the relative viscosity, η_r, defined as the ratio of the Newtonian viscosity of the composite to that of PA12 matrix, is plotted as a function of filler volume fraction in Figure 9.

In spite of some uncertainty in the determination of the relative viscosity, following the method proposed by Utracki and Lyngaae-Jorgensen,[30] the intrinsic viscosity $[\eta]$ and interaction constant k were determined by fitting the relative viscosity versus volume fraction curve to the second-order Einstein-type eq. (1):

$$\eta_r = 1 + [\eta]\phi + k(\eta\,[\phi])^2 \quad (1)$$

Knowing the intrinsic viscosity, the aspect ratio, p, defined as the ratio of particle diameter to the thickness of disk-like particles, can be inferred as follows:

$$[\eta] = 2.5 + 0.025\left(1 + p^{1.47}\right) \quad (2)$$

A least-square fit leads to $[\eta]$ and k values, which are reported in Table III. The values of p, estimated from eq. (2), are also presented in Table III.

Table III indicates that aspect ratio and interaction constant, which are equal to 200 and 0.8, respectively, for OMMT particles, are close to the values estimated by Aubry *et al.*[14] for OMMT/PA12 nanocomposites mixed with an internal mixer. The high aspect ratio of OMMT particles is the signature of partially exfoliated structure of OMMT particles within PA12 matrix.

Table III. Intrinsic Viscosity $[\eta]$, Interaction Constant, k, and Aspect Ratio, p, for OMMT, HARNT, and ST Fillers

	[η]	k	p
OMMT	65	0.8	200
HARNT	8	0.25	40
ST	18	0.7	80

On the contrary, HARNT particles are characterized by a much lower aspect ratio and interaction constant than those of OMMT particles, suggesting a rather microcomposite structure of HARNT particles within PA12 matrix.

Finally, intrinsic viscosity, aspect ratio, and interaction constant estimated for ST particles were shown to lie between those of OMMT and HARNT particles, in accordance with structural investigation. The relatively high aspect ratio of ST particles, ~80, is the mark of a nanostructure, which is close to that of OMMT/PA12 nanocomposites. However, in the case of ST particles, the nanostructure is affected by the presence of a few micrometric entities, as discussed above.

CONCLUSION

This study clearly shows that the twin-screw extruder is more adequate than the internal mixer, in the conditions we used, for the elaboration of synthetic talc/PA12 nanocomposites. Besides, structural characteristics of ST/PA12 nanocomposites, elaborated using a twin-screw extruder, are between those of OMMT/PA12 nanocomposites and HARNT/PA12 microcomposites. Actually, ST particles can be considered as potential challengers of OMMT, when dispersed in PA12 matrix, since they exhibit a mainly nanometric structure. However, the presence of a small amount of large particles (aggregates or agglomerates) in ST/PA12 nanocomposites, formed during the incorporation of materials into the mixing device, might reduce significantly some performances of these systems.

ACKNOWLEDGMENTS

The authors are grateful to Imerys Talc for logistic and financial support. We thank Philippe Eliès, François Michaud, Gérard Sinquin (Université de Bretagne Occidentale) for technical assistance in structural characterization and Christophe Cellard (Université de Bretagne Occidentale) for his kind help in extrusion camerawork.

REFERENCES

1. Sinha Ray, S.; Okamoto, M. *Prog. Polym. Sci.* **2003**, *28*, 1539.
2. Gilman, J. W. *Appl. Clay Sci.* **1999**, *15*, 31.
3. Zanetti, M.; Camino, G.; Thomann, R.; Mulhaupt, R. *Polymer* **2001**, *42*, 4501.
4. Tang, Y.; Hu, Y.; Wang, S.; Gui, Z.; Chen, Z. *Polym. Adv. Tech.* **2003**, *14*, 733.
5. Massersmith, P. B.; Giannelis, E. P. *J. Polym. Sci., Part A: Polym. Chem.* **1995**, *33*, 1047.
6. Ke, Z.; Yongping, B. *Mater. Lett.* **2005**, *59*, 3348.
7. Krook, M.; Albertsson, A. C.; Gedde, U. W.; Hedenqvist, M. S. *Polym. Eng. Sci.* **2004**, *42*, 1238.

8. Alexandre, M.; Dubois, P. *Mater. Sci. Eng.* **2000**, *28*, 1.
9. Reichert, P.; Kressler, J.; Thoann, R.; Mülhaupt, R.; Stöppelmann, G. *Acta Polym.* **1998**, *49*, 116.
10. Médéric, P.; Razafinimaro, T.; Aubry, T. *Polym. Eng. Sci.* **2006**, *46*, 986.
11. Usuki, A.; Kojima, Y.; Kawasumi, M.; Okada, K.; Fukushima, M.; Kurauchi, T.; Kamigaito, O. *J. Mater. Res.* **1993**, *8*, 1179.
12. Kojima, Y.; Usuki, A.; Kawasumi, M.; Okada, K.; Kurauchi, T.; Kamigaito, O.; Kaji, K. *J. Polym. Sci. Part B: Polym. Phys.* **1994**, *32*, 625.
13. Fornes, T. D.; Paul, D. R. *Macromolecules* **2004**, *37*, 7698.
14. Aubry, T.; Razafinimaro, T.; Médéric, P. *J. Rheol.* **2005**, *49*, 425.
15. Médéric, P.; Razafinimaro, T.; Aubry, T.; Moan, M.; Klopffer, M. H. *Macromolar Symposia* **2005**, *221*, 75.
16. Médéric, P.; Aubry, T.; Razafinimaro, T. *Int. Polym. Proc.* **2009**, *3*, 261.
17. Aït Hocine, N.; Médéric, P.; Aubry, T. *Polym. Test.* **2008**, *27*, 330.
18. Duska, J.; Fineston, A.; Maher, J. U.S. Pat. 4,626,557, **1986**.
19. Hong, C. H.; Lee, Y. B.; Bae, J. W.; Jho, J. Y.; Nam, J. O.; Hwang, T. W. *J. Appl. Polym. Sci.* **2005**, *98*, 427.
20. Leterme, P.; Gayot, A.; Finet, G.; Bizi, M.; Flament, M. P. *Int. J. Pharmac.* **2005**, *289*, 109.
21. Martin, F.; Ferret, J.; Lèbre, C.; Petit, S.; Grauby, O.; Bonino, J. P.; Arseguel, D.; Decarreau, A.; Ferrage, E. W.O. Pat. 2,008,009,799 A2, **2008**.
22. Martin, F.; Ferret, J.; Lèbre, C.; Petit, S.; Grauby, O.; Bonino, J. P.; Arseguel, D.; Decarreau, A.; Ferrage, E. W.O. Pat. 2008,009,800 A2, **2008**.
23. Martin, F.; Ferret, J.; Lèbre, C.; Petit, S.; Grauby, O.; Bonino, J. P.; Arseguel, D.; Decarreau, A.; Ferrage, E. W.O. Pat. 2,008,009,801 A2, **2008**.
24. Le Roux, C.; Martin, F.; Micoud, P.; Dumas, A. W.O. Pat. 2,013,004,979 A1, **2013**.
25. Dumas, A.; Martin, F.; Le Roux, C.; Micoud, P.; Petit, S.; Ferrage, E.; Brendlé, J.; Grauby, O.; Greenhill-Hopper, M. *Phys. Chem. Min.* **2013**, *40*, 361.
26. Yousfi, M.; Livi, S.; Dumas, A.; Le Roux, C.; Crépin Leblond, J.; Greenhill-Hooper, M.; Duchet-Rumeau, J. *J. Colloid Interface Sci.* **2013**, *403*, 29.
27. Paul, D. R.; Robeson, L. M. *Polymer* **2008**, *49*, 3187.
28. Bousmina, M.; Ait-Kadi, A.; Faisant, J. B. *J. Rheol.* **1999**, *43*, 415.
29. Fornes, T. D.; Yoon, P. J.; Keskkula, H.; Paul, D. R. *Polymer* **2001**, *42*, 9929.
30. Utracki, L. A.; Lyngaae-Jorgensen, J. *Rheol. Acta* **2002**, *41*, 394.